A 220 - 300 GHz Twin-FET Detector for Rotational Spectroscopy of Gas Mixtures

Muhammad Waleed Mansha, *Student Member, IEEE*, Timothy E. Rice, Matthew A. Oehlschlaeger, Ingrid Wilke and Mona M. Hella, *Senior Member, IEEE*

***Abstract*— In this paper, a twin-FET (field effect transistor) THz detector monolithically integrated with a dual-feed antenna is presented. The antenna-detector configuration can be extended for 'N' FET elements to relax the input impedance requirement for the detector readout circuitry while maintaining good responsivity. A dual-feed octagonal slot antenna is used to couple THz radiation and provide differential excitation to the twin-FET detector. The multi-feed antenna-FET detector interface can be designed for an arbitrary phase excitation of one or more FET elements. Fabricated in Global Foundries 22nm FD-SOI process, the proposed detector covers a measured frequency range from 220 GHz to 300 GHz. Such bandwidth is sufficiently wide to capture reliable spectral information for distinguishing a number of gases in a mixture. The absorption spectra of pure methanol, chloromethane and acetonitrile are measured using a rotational spectroscopy setup incorporating the twin-FET detector. Detection of a small concentration of acetonitrile, at 4 Torr pressure, is demonstrated in a binary mixture with predominantly chloromethane. Detection of ethanol and methanol in their binary mixture is also demonstrated at 4 Torr pressure. This is a significant step towards the development of all-electronic THz spectroscopy for the detection of volatile organic compounds (VOCs) in the presence of contaminants with a strong THz absorption signature at $>$ 1 Torr pressure.**

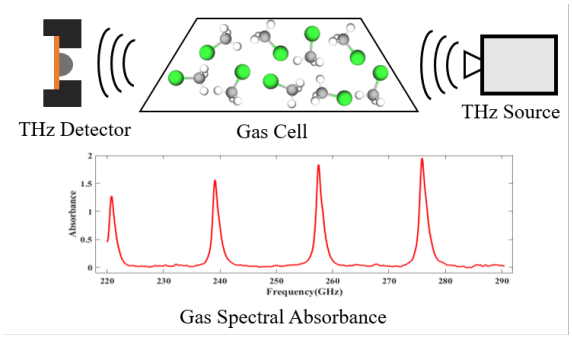

***Index Terms*— Antenna, detector, FDSOI, gas, mixture SOI, spectroscopy, terahertz, volatile-organic-compounds, wideband**

I. Introduction

THE detection and generation of terahertz (THz) wave signals is an active area of research with the potential for enabling a broad range of applications including ultra-high speed communication, imaging, instrumentation and sensing [1]. Being unaffected by smoke or dust particles, THz rotational absorption spectroscopy offers key advantages for the detection of volatile organic compounds (VOC) [2]. First, the absorption cross-section of molecules is larger for THz than for infrared photons. Second, the THz wave absorption spectra of molecules are highly specific and can be calculated analytically; even molecules that are structurally and chemically similar, can exhibit distinct THz wave absorption signatures. Finally, unlike electrochemical methods, rotational spectroscopy is a non-intrusive approach where the gaseous sample does not have to be in contact with the spectroscopic detection system. While rotational spectroscopy is a powerful analytical tool, however, the detection of non-polar molecules remains one of its limitations. Recently, chiral analysis has been proposed to allow for the detection of enantiomers. Such analysis has the potential to enhance the capabilities of rotational spectroscopy and enable its various applications [3].

Given its advantages, THz wave spectroscopy has been proposed as a method for the analysis of gases in the human breath to identify disease markers [4], [5]. While the spectra of pure compounds have been reported in [6]–[8], a gas sensor deployed in a practical setting will seldom encounter its target compound in a pure form. Thus gas sensors need to be robust enough to identify the target compound in the presence of contaminants which may or may not themselves have a THz wave absorption signature.

For the actual implementation of THz wave detection, several technology options are available that vary in terms of their sensitivity, specificity, size, cost and required operating conditions. Microbolometers offer the lowest noise performance along with high responsivity but require cryogenic temperatures for operation [9]. Golay cells and pyroelectric

This work is supported in part by the National Science Foundation Grant No.1851291. Chip Fabrication is sponsored by Global Foundries' university program for 22FDX technology.

M. W. Mansha, is with the Department of Electrical, Computer and Systems Engineering, Rensselaer Polytechnic Institute, Troy, NY 12180, USA (e-mail:manshm@rpi.edu).

T. E. Rice, is with the Department of Mechanical, Aerospace and Nuclear Engineering, Rensselaer Polytechnic Institute, Troy, NY 12180, USA (e-mail:ricet4@rpi.edu).

M. A. Oehlschlaeger, is with the Department of Mechanical, Aerospace and Nuclear Engineering, Rensselaer Polytechnic Institute, Troy, NY 12180, USA (e-mail:oehlsm@rpi.edu).

I. Wilke, is with the Department of Physics, Applied Physics and Astronomy, Rensselaer Polytechnic Institute, Troy, NY 12180, USA (e-mail:wilkei@rpi.edu).

M. M. Hella, is with the Department of Electrical, Computer and Systems Engineering, Rensselaer Polytechnic Institute, Troy, NY 12180, USA (e-mail:hellam@ecse.rpi.edu).

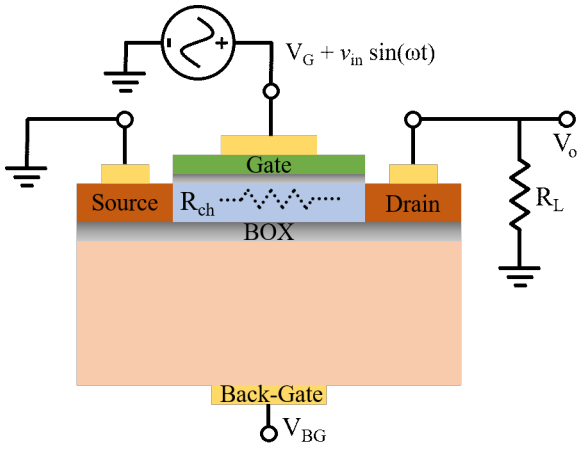

Fig. 1. Simplified structure of an FD-SOI FET detector.

detectors both have high responsivity to THz wave signals but they have a slow response time in the order of milliseconds [10], [11]. Schottky diodes present a good balance of relatively high responsivity along with fast response times [7], [12] but can be relatively costly. THz wave detectors using Field Effect Transistors (FETs) fabricated in standard silicon processes are compact and consume low power. Furthermore, the continuous development of advanced silicon technology nodes has enabled the design of single detectors as well as arrays of detectors at frequencies approaching 1 THz with good responsivity and fast response times [13], [14]. Rotational spectroscopy systems implemented with silicon integrated circuit based THz wave sources and detectors have been described in the literature; some examples include [8], [15]–[17]. There is however, still a need to develop THz sources and detectors that can span a wide frequency range, in the order of 100 GHz, to perform not only robust detection of pure gaseous samples but also for samples containing a number of absorbing gases.

There is a limited body of work on the detection of gas mixtures using THz wave spectroscopy. In [18], the detection of VOCs in the presence of a contaminant is reported while [19] demonstrated the detection of a mixture of VOCs is reported. However, these experiment were performed at very low, milli-Torr, pressure levels which requires specialized pumping equipment and hence these techniques are not suitable for the miniaturization required for many practical implementations. In [16], the detection of methanol in a mixture of nitrogen is demonstrated. However, nitrogen is almost transparent to THz wave signals and thus it is not established if the same detection could be performed in the presence of another THz wave absorbing species.

In this paper, we present (1) a wide-band THz detector based on twin FETs excited through an octagonal slot antenna, (2) a multi-port antenna-detector interface that allows for implementation of arbitrary phase excitation of one or more FET elements, (3) a rotational spectroscopy system employing the twin-FET detector, for spectroscopic detection of pure VOCs as well as their mixtures at above 1 torr pressure, where considerable pressure broadening effects increase the difficulty of classification of observed spectral data.

The design approach of the twin-FET detector can be extended to a detector with 'N' FET elements for increased tolerance to loading effects. The proposed antenna-detector configuration reduces the overall size of the detecting module and eliminates the losses associated with having a dedicated power splitter from the antenna to the FETs. The presented rotational spectroscopy system can operate between 220 GHz to 300 GHz. Such bandwidth is wide enough for robust detection of a variety of compounds. The rotational spectroscopy system is used to demonstrate the detection of absorbing gases in their binary mixtures at > 1 Torr pressure.

The paper is organized as follows: Section II describes the design of the THz detector. Section III characterizes the behavior of the THz detector and compares it to that of a standalone detector. In Section IV , the detector is integrated in a gas spectroscopy system and the results of spectroscopic measurements performed on pure samples of methanol, chloromethane and acetonitrile as well as those performed on a binary mixture of chloromethane and acetonitrile and ethanol and methanol are discussed.

II. Circuit Design

The FET detector's operating principle is based on the plasma wave theory proposed by Dyakanov-Shur [20], [21]. It can also be explained by the self-mixing of the input THz excitation using the non-linear response of the transistor [22].

If one considers the simple case of a single fully depleted silicon-on-insulator (FD-SOI) FET excited at the gate terminal with a THz wave signal as shown in Fig. 1, the maximum response of the detector $V_{det_{max}}$ can be represented by [23]:

$$v_{det_{max}} \approx \frac{e v_{in}^2}{4\eta k_b T}, \tag{1}$$

where e is the charge of an electron, v_{in} is the incident THz signal voltage, η is the ideality factor, k_b is the Boltzmann constant and T is the temperature. This peak response is achieved when the FET is biased in the sub-threshold region. It is worth noting that, while the above expression in (1) has been derived for heterostructure FETs, it was also validated for SOI FETs as in [24].

When an external load is connected to the output of the detector, the detector response is reduced from the maximum value predicted by (1). The load impedance represents the finite impedance of the readout circuitry or the amplifier stage following the detector. This loading effect can be explained using the voltage division between the FET channel resistance R_{ch} and the load impedance Z_L connected in series [25], [26].

$$V_o = \frac{Z_L}{Z_L + R_{ch}} v_{det} \tag{2}$$

Unless $R_{ch} \ll |Z_L|$, there is a considerable drop in the detector output V_o. R_{ch} depends on the biasing and the W/L ratio of the FET and can be in the order of tens of kilo ohms or more. Typical configurations for THz wave detection employ either an amplitude or a frequency modulated THz wave signal. When the modulation frequency is low, in the order of hundreds of kHz, high input impedance readout circuitry

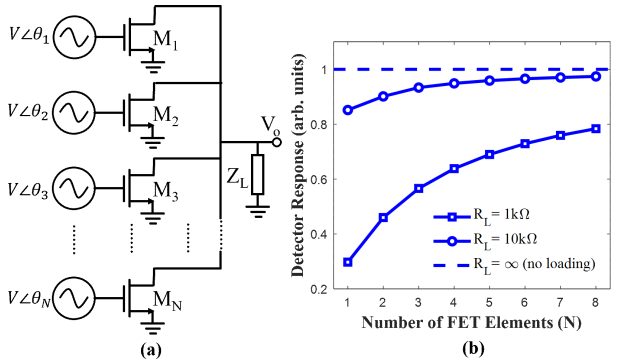

Fig. 2. (a) Schematic of a detector with 'N' FET elements for increased tolerance to detector loading (b) Simulated detector response as function of the number of parallel FET elements.

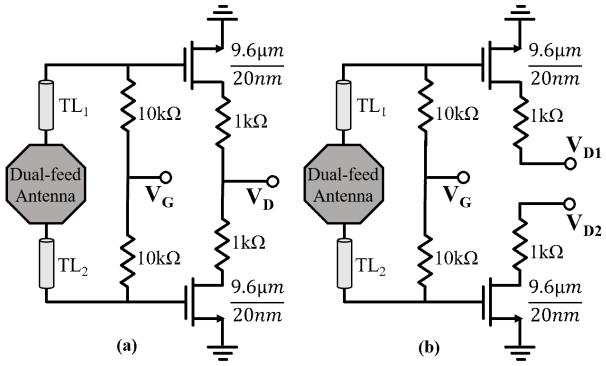

Fig. 3. (a) Schematic of the designed twin-FET THz detector. (b) Schematic of twin-FET detector with separate outputs for each FET.

can be easily implemented on chip [27], [28]. Increasing the modulation frequency to hundreds of MHz and above, reduces the effect of FET flicker noise, however, a high frequency amplifier should follow the detector. Such amplifiers tend to have a low input impedance, which would increase the effect of loading on the detector and reduce the strength of the detected signal. Note that, higher modulation frequency (at the order of several GHz) is also required in high data rate communication applications as reported in [29], [30].

To relax the input impedance requirement of the readout circuitry, rather than having a single FET, an array of $'N'$ parallel connected FET elements can be utilized, with the output extracted from the common drain terminal of all the transistors as shown in Fig. 2(a). This generalized architecture allows for arbitrary phase excitation of each FET element that may be provided through a N-feed antenna. In this arrangement, the effect of loading will be shared between the FET elements. The detector output can then be written as:

$$V_o = \frac{NZ_L}{NZ_L + R_{ch}} v_{det}, \tag{3}$$

Fig. 2(b) shows the simulated effect of loading on the detector response as a function of the number of FET elements $'N'$. It can be seen from the figure that the effect of loading is reduced as the number of FET elements are increased. Moreover, the reduction in loading is more significant when the detector interfaces with a load impedance comparable to or lower than the channel resistance of the FETs. It is worth noting that the idea of using two FETs connected to a differential antenna has been reported in prior art as in [28], however, in this paper, we propose the concept of multi-feed antenna that can provide signals with same amplitude but different phases depending on the number of antenna ports. The twin-FET detector is just a demonstration to validate the proposed concept. Theoretically having an array of $'N'$ FETs is possible, however, practically one has to consider applying the THz wave to each FET. One solution is to use an antenna array and couple each FET to its respective array element. This would translate to a large area specially on the lower side of the THz spectrum. A patch antenna at 250 GHz would occupy a chip area of $\sim$0.2 mm^2. Another solution would be to use one antenna and then a power splitter to feed each detector. Again, the losses in the power splitter as well as its size would affect the level of THz signal incident on each FET. The multi-feed antenna presented here couples THz power to each FET detector without any loss associated with power splitting or any size penalty when using an antenna array. Details on the antenna are given in section II-B.

A. FET Detector

The proposed THz wave detector is designed using two identical n-channel FETs with 20 nm gate lengths. A multi-fingered layout is utilized for each transistor with an effective total channel width of 9.6 μm. The transistors are sized by taking into consideration the flicker noise, channel resistance and the parasitic capacitance. Larger FETs have lower flicker noise and channel resistance but also have higher parasitic capacitance that can degrade the detector response and hence a compromise must be made. The drain terminals of the two transistors are tied together with 1 kΩ resistors. Differential input excitation is provided through a dual-feed octagonal slot antenna, in which the antenna outputs are tapped in a way to yield two received signal that are 180° out of phase. Each signal path from the antenna is fed to the gate of a transistor using a grounded coplanar waveguide (CPW). A symmetric layout is used throughout the design, with equal length of CPW line along each path to retain the 180° phase difference between the two THz signal inputs to the transistors. Fig. 3(a) shows the schematic of the designed twin-FET detector. 10 kΩ resistors connected to the gate of each transistor provide a path for biasing the transistor while preventing the leakage of the received THz signal towards the bias line. The THz response of the detector can be significantly enhanced when a small drain current is injected [31]. Biasing resistors provided at the drain terminals of the transistors allow the characterization of the detector in the presence of such biasing current. Access to the back gate bias voltage is provided through a DC pad, allowing an extra degree of freedom to tune the detector response post fabrication.

A second detector is also implemented which is identical to the designed twin-FET detector except the outputs from the two FETs are not connected together and are instead routed to individual pads. Fig. 3(b) shows the schematic of the second detector with separate output connections for each

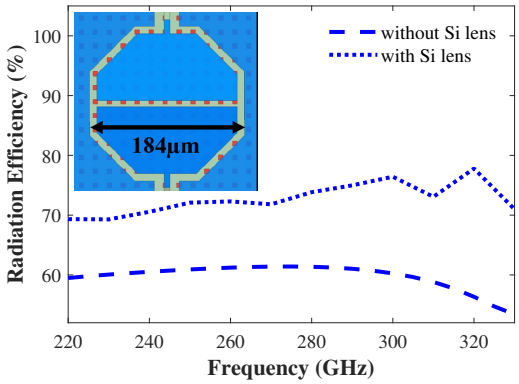

Fig. 4. Structure of the dual feed octagonal slot antenna and its simulated radiation efficiency with and without a silicon lens.

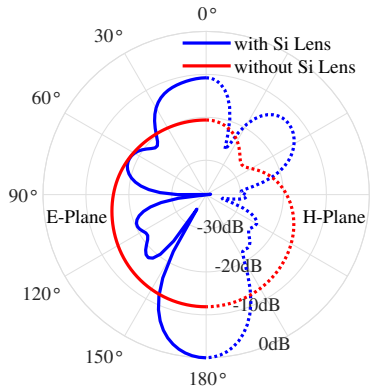

Fig. 5. Simulated E-plane and H-plane normalized radiation pattern of the dual-feed octagonal slot antenna with and without a silicon lens.

FET. When the output is measured from one of the FETs alone, it is equivalent to a conventional single FET detector. However, when V_{D1} and V_{D2} are connected together, the configuration simplifies to the twin-FET detector. Thus the detector in Fig. 3(b) can be used to compare the effect of loading on a single FET and twin-FET detector.

B. Dual-Feed Octagonal slot antenna

The overall usable bandwidth of the THz wave FET detector is limited by the bandwidth of the antenna. Examples of integrated wideband antenna topologies that don't require a specialized post processing step includes slot, dipole, monopole and stacked patch antennas [16], [32]–[34]. Other ultra wide band antenna structures such as log periodic multi-feed antennas [35], have curved periphery which is not compliant with the design rules of many large scale commercial IC processes. Here, an octagonal slot antenna is selected because of its wide bandwidth and commercial IC process compliant structure that lends itself well for adaptation to a multi-feed design. For an octagonal slot antenna, the electromagnetic field vector goes through a phase difference of 360° as one rotation is completed through the octagonal slots. Hence the location where the antenna outputs are tapped could be used to control the phase difference between the received outputs. In this design, only two opposite sides of the octagon are used to realize the excitation of the two transistors forming the detector. Similarly, a quad-feed octagonal slot antenna can also be designed while still maintaining symmetry between the antenna outputs [36]. This multi-feed antenna-FET detector interface can also be utilized for arbitrary phase excitation of one of more FET elements, paving the way for compact implementation of THz spectrometers as recently proposed in [37]. For the selected antenna, each arm will have a phase difference of 180°, so the FETs will receive THz radiation at different phases. However, since the FET acts as a broadband peak detector, the difference in phases will not affect the DC response.

The dual-feed octagonal slot antenna predominantly radiates from the bottom. The antenna is designed on the same thick copper metal layer as the signal lines of the grounded CPW to allow for seamless integration of the antenna and the transmission line. Inset in Fig. 4 shows the structure of the designed octagonal slot antenna, which occupies a chip area of 184 μm x 184 μm.

To minimize the lossy substrate waves excited due to backside radiation and to improve the radiation efficiency, the bottom of the detector chip is attached to a hyper hemispherical silicon lens. Three-dimensional (3D) electromagnetic (EM) simulation of the proposed antenna structure was performed in Ansys HFSS. Fig. 4 shows the simulated radiation efficiency of the octagonal slot antenna, with and without the silicon lens. As can be seen, in addition to improving the radiation efficiency, the silicon lens also significantly improves the antenna gain. Fig. 5 shows the simulated antenna radiation pattern, where it can be seen that the silicon lens, not only allows the antenna to receive more of the incident THz radiation but it also receives a greater portion of that power from the intended broadside downward direction. The top side radiation lobes are > 10 dB lower than the dominant back lobe of the antenna and thus the unintended top radiation of the antenna only has a minimal impact to the radiation efficiency in the intended downward direction. For the simulated results reported here, we assume a silicon lens with a diameter of 3 mm. This is mainly done due to the constraints imposed by the computational power and time required for electromagnetic simulations of large structures at THz frequencies. However, the trend observed from these simulations could be extended for silicon lenses of larger diameters.

III. Detector Characterization

The designed detector chips were fabricated using Global Foundries 22 nm FD-SOI process and each occupies a chip area of 590 μm x 340 μm including pads. Fig. 6 shows the chip micrographs, identifying the regions containing the antenna and the FETs. For testing, a high resistivity silicon wafer tile was bonded to the back side of the printed circuit board (PCB) which has a hole in the center. The chip is placed in the cavity formed by the PCB dielectric and the silicon wafer tile and wire bonded to the traces on the top side of the PCB. The PCB is then placed in a mount which contains a spring loaded 12 mm hyper-hemispherical silicon lens pushing onto the backside of the PCB. Because an epoxy is not used to keep the silicon lens in contact with

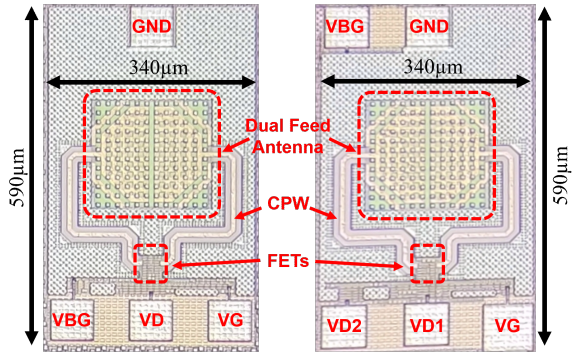

Fig. 6. Chip micrograph of the proposed THz detectors; Twin-FET detector (left), Twin-FET detector with separate outputs (right).

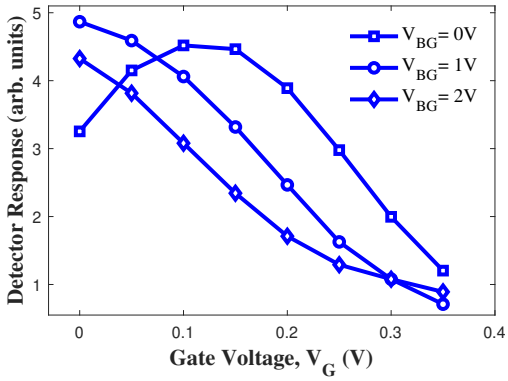

Fig. 8. Measured response of the detector versus gate voltage at 260 GHz for different values of the back gate voltage.

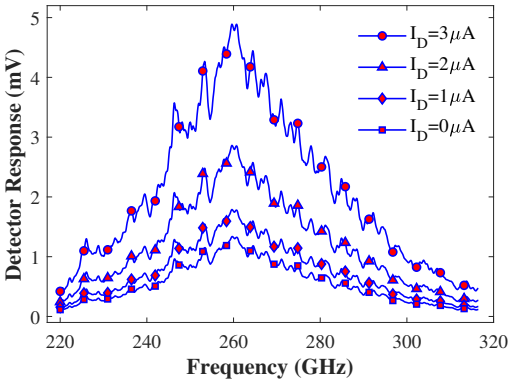

Fig. 7. Measured response of the detector for different values of the total drain current.

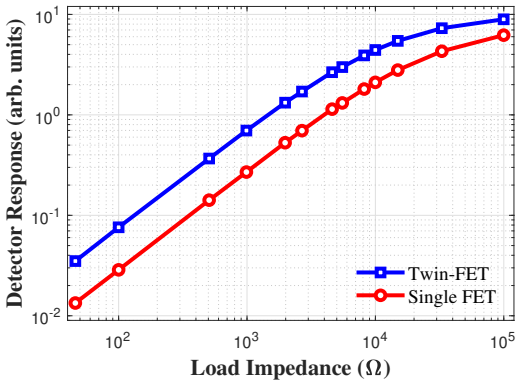

Fig. 9. Measured detector response at 260 GHz for a single FET and twin-FET detector configuration, as a function of the load impedance.

the chip, the relative position of the silicon lens and the chip can be varied for maximum received signal intensity. For the characterization of the detector, a Virginia Diodes WR 3.4 Frequency multiplier source is used. The input to the THz wave source is provided by an Anritsu 68369a/nv frequency synthesizer with a frequency sweep capability. A lock-in amplifier is used to extract the desired THz response from the voltage signal observed at the detector output.

Fig. 7 shows the detector response for different values of the total drain current supplied to the twin-FETs detector. It can be seen from the figure that the detector responds to THz signals over a broad frequency range from 220 GHz to over 300 GHz. This bandwidth is sufficient to observe multiple absorption peaks for a variety of VOCs as validated recently in [38]. The partial reflection of the incident THz wave signal from the silicon lens-silicon tile and silicon tile-chip interfaces leads to interference patterns, which can be seen as oscillations in the measured detector response. The voltage response of the detector can be significantly enhanced by increasing the drain bias current [31]. However, the added current also increases the noise contribution of the detector, which does not translate to any improvement in the signal-to-noise ratio (SNR). Instead, optimization of transistor sizing can be done to achieve the desired balance between responsivity and noise performance [39].

Fig. 8 shows the variation of the detector response at the mid-band frequency of 260 GHz as a function of the biasing gate voltage 'V_G'. The response is plotted for different values of the back gate voltage 'V_{BG}'. The detector response curves move towards lower gate voltages as the back-gate voltage V_{BG} is increased. This can be explained by the modulation of the threshold voltage of the FET by the back gate voltage [40]. The back-gate bias can be utilized to tune the detector response, compensating for the threshold voltage variations observed across different chips.

The effect of loading was characterized by using the second detector with two separate outputs and connecting controlled impedances in parallel with the lock-in amplifier. Due to the large 100 MΩ input impedance of the lock-in amplifier, the effective load impedance seen by the detector is the relatively small impedance connected in parallel. For each load impedance, the detector response at 260 GHz was recorded for a single FET and for the two FET outputs connected together. Fig. 9 shows the measured detector response as a function of the load impedance. The detector response decreases when the load impedance decreases but it can be seen that the twin-FET configuration achieves consistently higher detector response compared to the single-FET configuration.

The inherent noise of the detectors was characterized using a SR770 spectrum analyzer. Fig. 10 shows the measured voltage noise spectral density of the single FET and twin-

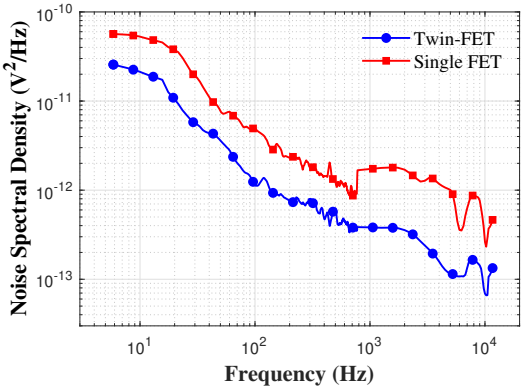

Fig. 10. Measured voltage noise spectral density of the single-FET and twin-FET detector.

FET detectors. For the noise measurements, the detectors were biased at the gate for maximum responsivity, and at the drain with a small fixed voltage of 20 mV. Spurs in the DC bias, originating from the 60 Hz AC supply and its harmonics were filtered from the measurements. The noise contribution of the detectors is dominated by flicker noise at low frequency offsets. Thus the measured voltage noise spectral density has a decreasing trend with frequency. Moreover, the twin-FET detector has a lower noise spectral density than the single FET detector. The lower noise of the twin-FET detector can be explained by its larger effective area than the single FET detector.

IV. Rotational Spectroscopy using the Twin-FET Detector

For demonstration of rotational gas spectroscopy, a measurement setup similar to the one described in our earlier publication [16] is utilized. The specially designed gas cell with 45° angled windows is only 21.6 cm which is significantly shorter than other spectroscopy works that have utilized gas cells with length $\geq$ 0.7 m [15], [18], [41]. Fig. 11 shows the actual photo of the spectroscopic measurement setup. The THz signal is amplitude modulated at 3 kHz, limited by the capabilities of the THz wave source. Spectral resolution of the measurement system is limited to the resolution of the RF signal sweeper times the multiplication factor of the THz wave source. The THz wave source and detector are positioned at the focal points of the Teflon lenses. The overall distance between the THz wave source and detector is approximately 1 m. The diverging THz radiation beam emitted by a horn antenna, connected to the THz wave source, is collimated using a Teflon lens and passes through the gas cell. After passing through the gas cell, the THz radiation beam is focused on the detector using another identical Teflon lens. The output signal from the detector is fed to a lock-in amplifier which extracts the THz wave response.

Gases are identified by their absorption of THz wave photons at specific frequencies. To determine the absorbance, the baseline signal without the absorbing gas 'I_o' and the response of the detector when the gas is present and held at a controlled pressure inside the gas cell 'I_g', are measured.

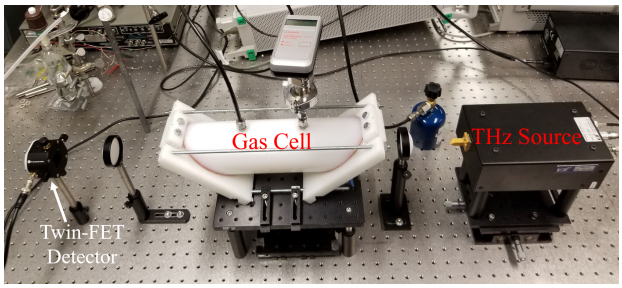

Fig. 11. Photograph of the spectroscopic measurements setup.

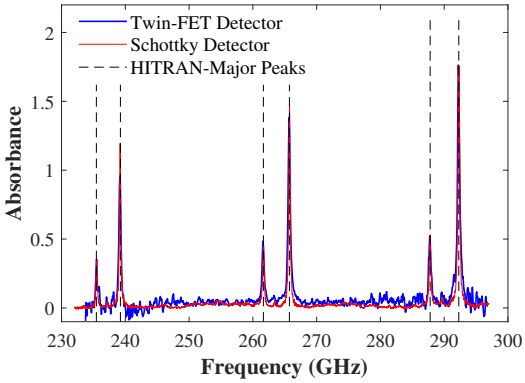

Fig. 12. Measured spectral absorbance of chloromethane at 2 Torr pressure using the proposed THz detector as well as a commercial Schottky diode detector. HITRAN predicted major absorbance peak locations are also annotated.

Using the two measured responses, the spectral absorbance of a gas can be calculated as:

$$Absorbance = A = -ln\left(\frac{I_o}{I_g}\right) \tag{4}$$

Each spectral scan was done at a sweep rate of approximately 1 GHz/s. However, recent experimentation has shown that even faster scan rates can be utilized without any degradation in the measured spectral absorbance. Ideally the spectral measurements are desired to be performed as close as possible to the atmospheric pressure to minimize the pumping requirement. However, at higher pressures, line broadening effects distort the characteristic spectral transitions of molecules. That is why reported works on detection of gas mixtures using rotational spectroscopy have utilized very low, milli-torr pressure levels [18], [19].

A rotational spectroscopy based sensor may be employed to detect its target compound in very low ppm concentration such as in air quality monitoring to very high concentrations approaching 100% purity such as relative concentration monitoring of reactants in chemical industry. The concentrations tested here serve as a proof of concept for detection of multiple absorbers at $>$ 1 torr pressure.

The frequency range between 220 GHz and 300 GHz does not contain any strong absorption peak of water vapors [42] which can dominate the relatively weak absorption peaks of some compounds. Moreover, this band has characteristic absorption peaks for a variety of compounds [38] and is thus

TABLE I
APPROXIMATE FREQUENCY BETWEEN CONSECUTIVE ABSORPTION PEAKS FROM 220 GHZ TO 300 GHZ*

Compound	Approx. frequency between consecutive absorption peaks (GHz)
Acetaldehyde	19
Acetonitrile	19
Ethanol	16
Methanol	10
Formaldehyde	9
Chloroform	7
Chloromethane	4
Formic acid	3

*Extracted from measurements reported in [38].

suitable for spectroscopic applications. The robust detection of a compound requires that more than one absorption peak of that compound be measured by the spectroscopic detection system. The spectra of various VOCs of interest have been reported in the frequency band of interest [38]. The approximate frequency between two consecutive absorption peaks of compounds has been extracted from spectral measurements and is shown in Table. I. The 80 GHz usable bandwidth of the twin-FET detector is thus sufficient to robustly detect a variety of compounds.

A. Detection of Pure Gases

Fig. 12 shows the measured spectral absorbance of Chloromethane (CH_3-Cl) at 2 Torr pressure. The measured absorbance using the proposed detector is compared to a commercially available Schottky diode detector from Virginia Diodes Inc. It can be seen from the figure that there is good correlation between the measured spectra and the location of the absorption peaks is consistent with those predicted by the HITRAN database (High-Resolution Transmission Molecular Absorption Database). The detector was also used to catalog the absorption spectra of a gas at different pressures. For spectroscopic detection, the sensitivity of the system is limited by the absorbance noise floor. The absorbance noise floor is a function of the detector noise and is calculated as the absorbance of any two consecutive baselines sweeps performed using the detector. Fig. 13 shows the measured absorption spectra of pure acetonitrile (CH_3-CN) at 1 torr and 4 torr pressure along with the absorbance noise floor. As can be seen, there is no shift in the location of the major absorption peak and the pressure broadening of absorption peaks is observed. The inset in the figure shows a subset of the plot, zoomed in at the absorbance noise floor.

We can reliably detect a compound if the absorbance noise floor of the system is significantly below the peak absorbance of the compound, or:

$$-\,log\left(\frac{I-N_{max}}{I+N_{max}}\right) \ll A, \tag{5}$$

where, I is the voltage response of the detector in the absence of noise, N_{max} is the maximum noise voltage and A is the peak absorbance of the compound to be detected. This translates to a constraint on the minimum signal-to-noise ratio ($SNR_{min} = I^2/N_{max}^2$) of the system.

$$SNR_{min} \gg \left(\frac{10^A+1}{10^A-1}\right)^2. \tag{6}$$

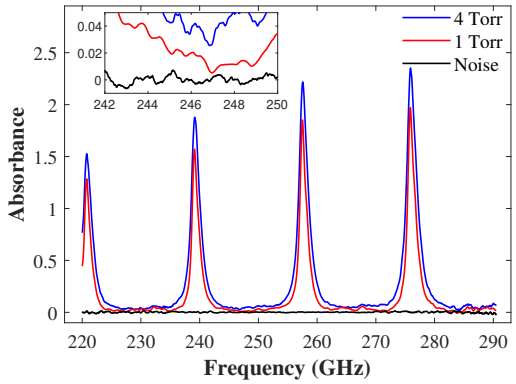

Fig. 13. Measured spectral absorbance of pure acetonitrile using the differential FET detector at two different pressures and the absorbance noise floor.

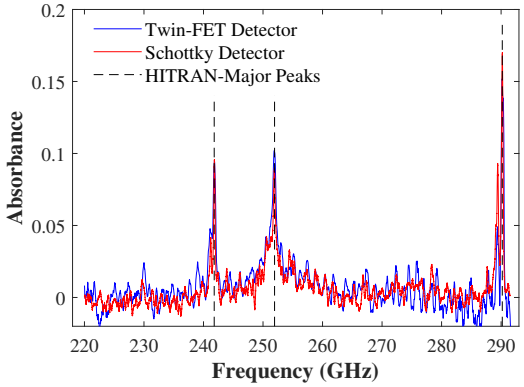

Fig. 14. Measured spectral absorbance of methanol at 2 Torr pressure using the differential FET detector and a commercial Schottky diode detector. HITRAN predicted major absorbance peak locations are annotated.

Methanol is a relatively weak absorber of THz wave radiation and is thus harder to detect. It has two characteristic absorption peaks between 235 GHz and 245 GHz that have an expected absorbance of ~0.1 at 2 Torr pressure. From (6), reliable detection of these absorption peaks requires that $SNR_{min} \gg 76$ for the detection system. Fig. 14 shows the measured spectral absorbance of Methanol (CH_3-OH) at 2 Torr pressure. It can be seen from Fig. 14 that the major absorbance peaks of Methanol were identified by the spectral measurements done with the twin-FET detector and the detected peaks are significantly above the absorbance noise level. The spectral absorbance is in good correlation with the commercial Schottky detector, that has a typical responsivity and noise equivalent power (NEP) of 500 V/W and 10 $pW/\sqrt{Hz}$ respectively [43]. Moreover, the spectral location of the measured absorbance peaks more accurately matches the HITRAN predictions than the measured data from the FET detector reported in [16].

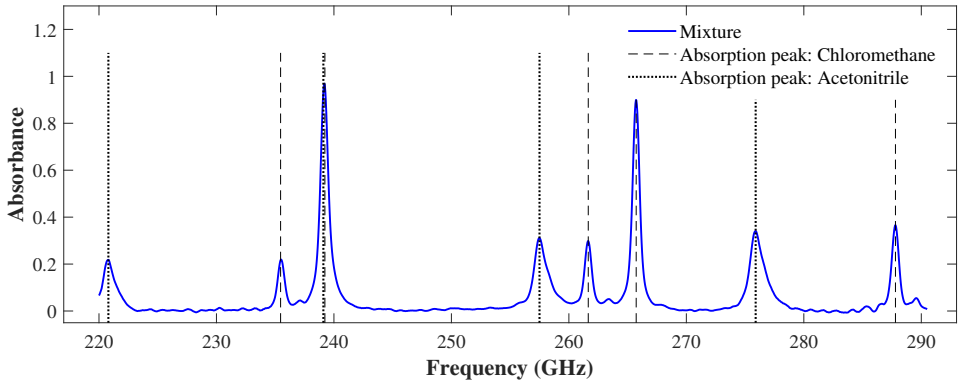

Fig. 15. Measured spectral absorbance of a mixture of chloromethane and acetonitrile. The absorption peak locations of pure acetonitrile and pure chloromethane are annotated.

B. Detection of Gases in a Mixture

Rotational spectroscopy is a robust technique which is not only useful for characterizing pure gases but can also be used for qualitative identification of gases in a mixture. Fig. 15 shows the measured spectral absorbance of a mixture of approximately 88% chloromethane and 12% acetonitrile held at 4 Torr total pressure. It can be seen from the figure that absorption peaks at frequencies identified by the pure absorption spectra of acetonitrile and chloromethane are also visible in the spectral absorbance of their mixture and therefore can be used for the identification of these gases. It is interesting to note that both chloromethane and acetonitrile have an absorption peak around 239 GHz. In the absorption spectra of the mixture, those two absorption peaks have merged into a single peak. If narrow band spectroscopy systems, as in [15]–[17], were utilized for this measurement, the presence of the small amount of acetonitrile in the mixture would have been missed. Similar conclusions can be drawn from the results of a spectroscopic measurements performed on a binary mixture of 60:40 ethanol and methanol at 4 Torr pressure as shown in Fig. 16. Methanol and ethanol both have a strong characteristic absorption peak around 242 GHz. In absorption of the mixture, the two peaks merge into one peak. However, since a wide frequency scan was performed which captured multiple absorption peaks for each compound, their presence could still be identified in the mixture.

Based on the above measurement results, one can conclude that the capability to scan a wide frequency range in the order of tens of GHz, is vital for the robust identification of gases in a mixture. Even if two gasses in a sample may have one absorption peak close to another, it is highly unlikely that they would have multiple peaks at identical or sufficiently close frequencies. It is also worth mentioning that if the absorption spectra of the mixture are measured at lower pressures, the single merged absorption peak would split up into the individual absorption peak corresponding to each of the pure samples.

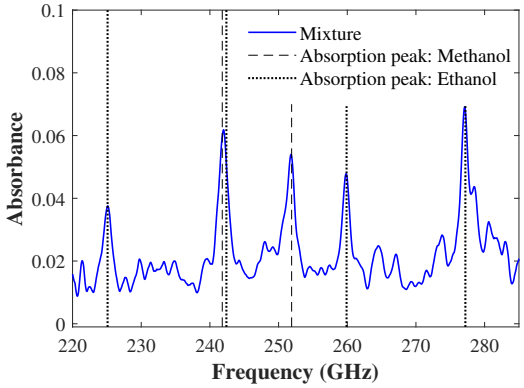

Fig. 16. Measured spectral absorbance of a mixture of ethanol and methanol at 4 Torr. The absorption peak locations of pure ethanol and pure methanol are annotated.

V. Conclusion

The design and implementation of a twin-FET THz wave detector in 22 nm FD-SOI technology is described. The detector is coupled to a broadband, compact and dual-feed octagonal slot antenna. The advantages and feasibility for the extension of the proposed detector topology to one with higher number of FET elements were discussed. The implemented twin-FET detector is characterized from 220 GHz to 300 GHz and is shown to be more resistant to loading than a single FET detector. The twin-FET detector is utilized to measure the THz absorption spectra of pure samples of methanol, acetonitrile and chloromethane. As a step towards the implementation of a practical gas sensor based on rotational spectroscopy, the implemented twin-FET detector is employed to demonstrate the detection of chloromethane-acetonitrile and ethanol-methanol in their respective binary mixture.

Acknowledgment

The authors would like to acknowledge the National Science Foundation for sponsoring this research work through the research grant No. 1851291 and Global Foundries for providing silicon fabrication through the 22FDX university program. The authors would also like to thank Prof. Michael Shur for the helpful discussions into the physics of THz detection using FETs, Dr. Silke Bargstaedt-Franke for helpful discussions on microchip fabrication and Mr. Junsung Park for assisting with detector noise measurements.

REFERENCES

[1] P. Hillger, J. Grzyb, and U. R. Pfeiffer, "Terahertz imaging and sensing applications with silicon-based technologies," *IEEE Trans. THz Sci. Technol.*, vol. 9, no. 1, pp. 1–19, Jan 2019.

[2] Y. Hsieh *et al.*, "Dynamic terahertz spectroscopy of gas molecules mixed with unwanted aerosol under atmospheric pressure using fibre-based asynchronous-optical-sampling terahertz time-domain spectroscopy," *Sci. Reports*, vol. 6, p. 28114, Jun 2016.

[3] B. Pate *et al.*, "A chiral tagging strategy for determining absolute configuration and enantiomeric excess by molecular rotational spectroscopy," in *72nd International Symp. on Molecular Spectroscopy*, 2017, pp. 1–1.

[4] I. R. Medvedev *et al.*, "Analysis of exhaled human breath via terahertz molecular spectroscopy," in *41st International Conf. on Infrared, Millimeter, and Terahertz waves (IRMMW-THz)*, 2016, pp. 1–2.

[5] N. Rothbart, K. Schmalz, J. Borngraber, S. B. Yilmaz, D. Kissinger, and H. Hubers, "Towards breath gas detection with a 245 GHz gas sensor based on SiGe BiCMOS technology," in *2017 IEEE SENSORS Conf.*, 2017, pp. 1–3.

[6] C. Wang and R. Han, "Dual-terahertz-comb spectrometer on CMOS for rapid, wide-range gas detection with absolute specificity," *IEEE J. Solid-State Circuits*, vol. 52, no. 12, pp. 3361–3372, Dec 2017.

[7] A.Tekawade *et al.*, "Towards realization of quantitative atmospheric and industrial gas sensing using THz wave electronics," *App. Phy. B*, vol. 124, no. 6, pp. 105–115, May 2018.

[8] N. Rothbart, K. Schmalz, and H. Hubers, "Gas spectroscopy at 222 – 270 GHz based on SiGe BiCMOS using a multi-pass ring cell," in *44th International Conf. on Infrared, Millimeter, and Terahertz Waves (IRMMW-THz)*, 2019, pp. 1–2.

[9] T. Otsuji, "Trends in the research of modern terahertz detectors: Plasmon detectors," *IEEE Trans. THz Sci. Technol.*, vol. 5, no. 6, pp. 1110–1120, 2015.

[10] Tydex, "Golay detectors," [online], Available: http://www.tydexoptics.com/pdf/Golay_Detectors.pdf, Accessed on: Apr 4, 2020.

[11] A. Rogalski and F. Sizov, "Terahertz detectors and focal plane arrays," *Opto-Electron. Rev.*, vol. 19, no. 3, pp. 346–404, Sep 2011.

[12] A.Tekawade *et al.*, "Towards industrial THz wave electronic gas sensing and spectroscopy," in *44th International Conf. on Infrared, Millimeter, and Terahertz waves (IRMMW-THz)*, 2019, pp. 1–2.

[13] R. Jain, R. Zatta, J. Grzyb, D. Harame, and U. R. Pfeiffer, "A terahertz direct detector in 22nm FD-SOI CMOS," in *2018 13th European Microwave Integrated Circuits Conf. (EuMIC)*, 2018, pp. 25–28.

[14] D. Y. Kim, S. Park, R. Han, and K. O. Kenneth, "Design and demonstration of 820-GHz array using diode-connected NMOS transistors in 130-nm CMOS for active imaging," *IEEE Trans. THz Sci. Technol.*, vol. 6, no. 2, pp. 306–317, 2016.

[15] N. Rothbart, K. Schmalz, J. Borngraber, D. Kissinger, and H. Hubers, "Gas spectroscopy by voltage-frequency tuning of a 245 GHz SiGe transmitter and receiver," *IEEE Sensors J.*, vol. 16, no. 24, pp. 8863–8864, Dec 2016.

[16] M. W. Mansha, K. Wu, T. E. Rice, M. A. Oehlschlaeger, M. M. Hella, and I. Wilke, "Detection of volatile organic compounds using a single transistor terahertz Detector implemented in standard BiCMOS technology," in *2019 IEEE SENSORS Conf.*, 2019, pp. 1–4.

[17] A. Tang, B. Drouin, Y. Kim, G. Virbila, and M. F. Chang, "95–105 GHz 352 mW all-silicon cavity-coupled pulsed echo rotational spectroscopy system in 65 nm CMOS," *IEEE Trans. THz Sci. Technol.*, vol. 7, no. 3, pp. 244–249, May 2017.

[18] Q. Zhong *et al.*, "225–280 GHz receiver for rotational spectroscopy," in *2016 IEEE Radio Frequency Integrated Circuits Symp. (RFIC)*, May 2016, pp. 298–301.

[19] C. F. Neese, I. R. Medvedev, G. M. Plummer, A. J. Frank, C. D. Ball, and F. C. De Lucia, "Compact submillimeter/terahertz gas sensor with efficient gas collection, preconcentration, and ppt sensitivity," *IEEE Sensors J.*, vol. 12, no. 8, pp. 2565–2574, 2012.

[20] M. Dyakonov and M. Shur, "Shallow water analogy for a ballistic field effect transistor: New mechanism of plasma wave generation by dc current," *Phys. Rev. Lett.*, vol. 71, no. 15, pp. 2465–2468, Oct 1993.

[21] ——, "Detection, mixing, and frequency multiplication of terahertz radiation by two-dimensional electronic fluid," *IEEE Trans. Electron Devices*, vol. 43, no. 3, pp. 380–387, 1996.

[22] A. Lisauskas, U. Pfeiffer, E. Öjefors, P. H. Bolìvar, D. Glaab, and H. G. Roskos, "Rational design of high-responsivity detectors of terahertz radiation based on distributed self-mixing in silicon field-effect transistors," *J. App. Phy.*, vol. 105, no. 11, p. 114511, 2009.

[23] W. Knap *et al.*, "Nonresonant detection of terahertz radiation in field effect transistors," *J. App. Phy.*, vol. 91, no. 11, pp. 9346–9353, 2002.

[24] N. Pala, F. Teppe, D. Veksler, Y. Deng, M. S. Shur, and R. Gaska, "Nonresonant detection of terahertz radiation by silicon-on-insulator MOSFETs," *Electronics Letters*, vol. 41, no. 7, pp. 447–449, 2005.

[25] W. Stillman, M. S. Shur, D. Veksler, S. Rumyantsev, and F. Guarin, "Device loading effects on nonresonant detection of terahertz radiation by silicon MOSFETs," *Electronics Letters*, vol. 43, no. 7, pp. 422–423, March 2007.

[26] M. Sakowicz *et al.*, "Terahertz responsivity of field effect transistors versus their static channel conductivity and loading effects," *J. App. Phy.*, vol. 110, no. 5, p. 054512, 2011.

[27] A. Boukhatma *et al.*, "A 533pW NEP 31×31 pixel THz image sensor based on in-pixel demodulation," in *40th European Solid State Circuits Conf. (ESSCIRC)*, 2014, pp. 303–306.

[28] E. Ojefors, U. R. Pfeiffer, A. Lisauskas, and H. G. Roskos, "A 0.65 THz focal-plane array in a quarter-micron CMOS process technology," *IEEE J. Solid-State Circuits*, vol. 44, no. 7, pp. 1968–1976, 2009.

[29] K. Wu, G. Ducournau, and M. M. Hella, "A 240 GHz receiver with 6 Gb/s data rate based on plasma wave detection in sige technology," in *2019 44th International Conf. on Infrared, Millimeter, and Terahertz Waves (IRMMW-THz)*, 2019, pp. 1–2.

[30] K. Wu *et al.*, "A 300 GHz data communication receiver using plasma-wave fet detector in 65nm CMOS," in *2020 IEEE Radio and Wireless Symposium (RWS)*, 2020, pp. 72–75.

[31] D. Veksler, F. Teppe, A. P. Dmitriev, V. Y. Kachorovskii, W. Knap, and M. S. Shur, "Detection of terahertz radiation in gated two-dimensional structures governed by dc current," *Phys. Rev. B*, vol. 73, p. 125328, 2006.

[32] Z. Hu, C. Wang, and R. Han, "A 32-unit 240-GHz heterodyne receiver array in 65-nm CMOS with array-wide phase locking," *IEEE J. Solid-State Circuits*, vol. 54, no. 5, pp. 1216–1227, 2019.

[33] A. Mostajeran, A. Cathelin, and E. Afshari, "A 170-GHz fully integrated single-chip FMCW imaging radar with 3-D imaging capability," *IEEE J. Solid-State Circuits*, vol. 52, no. 10, pp. 2721–2734, 2017.

[34] D. Fritsche, P. Stärke, C. Carta, and F. Ellinger, "A low-power SiGe BiCMOS 190-GHz transceiver chipset with demonstrated data rates up to 50 Gbit/s using on-chip antennas," *IEEE Trans. Microw. Theory Techn.*, vol. 65, no. 9, pp. 3312–3323, 2017.

[35] X. Wu and K. Sengupta, "On-chip THz spectroscope exploiting electromagnetic scattering with multi-port antenna," *IEEE J. Solid-State Circuits*, vol. 51, no. 12, pp. 3049–3062, 2016.

[36] M. W. Mansha and M. Hella, "A 7.4dBm EIRP, 20.2% DC-EIRP efficiency 148 GHz coupled loop oscillator with multi-feed antenna in 22nm FD-SOI," in *2020 IEEE Radio Frequency Integrated Circuits Symposium (RFIC)*, 2020.

[37] X. Liu, T. Ytterdal, and M. Shur, "Plasmonic fet terahertz spectrometer," *IEEE Access*, vol. 8, pp. 56 039–56 044, 2020.

[38] T. E. Rice, M. A. Z. Chowdhury, M. W. Mansha, M. M. Hella, I. Wilke, and M. A. Oehlschlaeger, "VOC gas sensing via microelectronics-based absorption spectroscopy at 220–330 GHz," *App. Phy. B*, vol. 126, no. 9, pp. 152–164, 2020.

[39] R. Tauk *et al.*, "Plasma wave detection of terahertz radiation by silicon field effects transistors: Responsivity and noise equivalent power," *App. Phy. Lett.*, vol. 89, no. 25, p. 253511, 2006.

[40] H. K. Lim and J. G. Fossum, "Threshold voltage of thin-film silicon-on-insulator (SOI) MOSFET's," *IEEE Trans. Electron Devices*, vol. 30, no. 10, pp. 1244–1251, Oct 1983.

[41] C. Wang and R. Han, "Dual-terahertz-comb spectrometer on cmos for rapid, wide-range gas detection with absolute specificity," *IEEE J. Solid-State Circuits*, vol. 52, no. 12, pp. 3361–3372, 2017.

[42] R. J. Emery and A. M. Zavody, "Atmospheric propagation in the frequency range 100-1000 ghz," *Radio and Electronic Engineer*, vol. 49, no. 7.8, pp. 370–380, 1979.

[43] V. Inc., "Quasi-optical broadband detectors," [online], Available: https://www.vadiodes.com/VDI/pdf/2009AugustNews.pdf, Accessed on: Jun 13, 2020,.

Muhammad Waleed Mansha received the B.Sc. degree in electrical engineering from University of Engineering and Technology Lahore, Pakistan, in 2015 and and M.S. degree in electrical engineering from Rensselaer Polytechnic Institute, USA in 2019. He is currently pursuing a Ph.D. degree in electrical engineering at Rensselaer Polytechnic Institute, USA.

He was an intern at Mixcomm Inc. in 2018 and Nokia Bell Labs in 2020 where he worked on circuit blocks for millimeter-wave transceivers. His research interests include integrated circuit techniques for signal generation and detection in the millimeter wave and THz band.

Mr. Mansha was the recipient of the IEEE SENSORS Conference Best Student Paper Award in 2019 and the Rensselaer Founders Award of Excellence in 2018.

Timothy E. Rice received the B.S. degree in aerospace engineering from Syracuse University, USA in 2017. He is currently pursuing a Ph.D. degree in aerospace engineering at Rensselaer Polytechnic Institute, USA.

His research interests are in the study of the rotational spectrum of polar gaseous compounds using mm-wave transmitters and receivers and its application to gas sensing techniques.

Matthew A. Oehlschlaeger received the received a B.S. in mechanical engineering from Virginia Tech (2000), and M.S. (2002) and Ph.D. (2005) degrees in mechanical engineering from Stanford University.

He joined the faculty at Rensselaer in 2006, where since 2014 he has served as the Associate Dean for Academic Affairs within the School of Engineering and as a Professor of Mechanical and Aerospace Engineering. His research focuses on gas sensor development, chemical kinetics, and combustion. He has co-authored approximately 100 papers, led government- and industrial-funded research programs, and garnered several national awards, including the Presidential Early Career Award for Scientists and Engineers (PECASE).

Dr. Oehlschlaeger is a Fellow of the American Society of Engineers (ASME) and serves as an Associate Editor for the International Journal of Fuels and Lubricants and the Journal of Thermal Science and Engineering Applications.

Ingrid Wilke received the M.S. degree in physics from the University at Albany - State University of New York - in 1986, the Diploma degree in physics from the Julius-Maximilians-Universiy Wuerzburg, Germany, in 1988, the Ph.D. degree in physics from ETH Zuerich, Switzerland in 1993, and the Habilitation in experimental physics from the University of Hamburg, Germany, in 2002.

She is currently an Associate Professor of Physics in the Department of Physics, Applied Physics & Astronomy. Her research interest includes ultrafast laser applications, and THz wave science & technology with emphasis on THz wave sources, detectors, and system applications, as well as materials properties in the THz wave frequency band.

Mona M. Hella (Senior Member, IEEE) received the B.Sc. and M.Sc. degrees in electronic and communications engineering from Ain Shams University, Cairo, Egypt, and the Ph.D. degree in electrical engineering from The Ohio State University, Columbus, OH, USA, in 2001.

From 2001 to 2003, she was with RF Micro Devices Inc. (now Qorvo), Billerica, MA, USA, working on optical communication circuits and silicon-based wireless systems. She joined the Electrical, Computer and Systems Engineering Department, Rensselaer Polytechnic Institute, Troy, NY, USA, in 2004, where she is currently a Professor. She was the Sensors Thrust Leader of the National Science Foundation Engineering Research Center (ERC) on Light Enabled Systems and Applications (LESA) (2010 – 2018). She coauthored two books: Power Management Integrated Circuits and Technologies (CRC Press, Taylor and Francis Group, 2016) and RF CMOS Power Amplifier, Theory, Design, and Implementation (Kluwer Academic Publishers, 2002), three book chapters, and published over 100 peer-reviewed conference and journal publications. Her research interests include the areas of mm-wave, THz circuits and systems, and integration platforms for biomedical sensing and energy harvesting applications.

Dr. Hella serves on the Technical Program and Steering Committees of the Radio Frequency Integrated Circuits (RFIC) Symposium, the Midwest Symposium on Circuits and Systems (MWSCAS), and the Optical Fiber Communication (OFC) Conference. She was Fulbright Scholar in 2015, and has served as an Associate Editor for the IEEE trans. on Very Large Scale Integration from 2011 to 2014, and the IEEE trans. on Circuits and Systems-I since 2019.